



## **Laser ultrasonics applied to surface and subsurface flaws detection in sphere, example of c-crack detection in nitride ceramic bearing balls**

Arnaud VANHOYE <sup>1</sup>, Philippe BREDIF <sup>1</sup>, Laurent SCHWEITZER <sup>2</sup>

<sup>1</sup> Commissariat à l'Énergie Atomique, France, [arnaud.vanhoye@cea.fr](mailto:arnaud.vanhoye@cea.fr)

<sup>2</sup> Safran Aircraft Engines, Villaroche, France, [laurent.schweitzer@safrangroup.com](mailto:laurent.schweitzer@safrangroup.com)

### **Abstract**

The generation and detection of ultrasound using laser is not widespread in industry as it remains a costly technology while constraining due to security aspects. However, it constitutes one of the only efficient means to generate ultrasound contactless, and is thus well suited for very specific applications such as hot piece inspection or complex geometry inspection. Contactless generation and detection is also a major benefit for surface waves applications, as the detection measurement will not alter the wave propagation phenomena.

Based on these assets, an inspection method dedicated to surface and subsurface flaw detection in spherical elements such as bearing balls is proposed. The method uses the propagation of Rayleigh waves confined to the sphere equator and extracts flaw signature thanks to a specific signal processing algorithm. The method is a potential solution for the inspection of ceramic bearing balls, which is of crucial importance for aeronautic industry as they ensure the proper functioning of jet engine.

The developed method is evaluated for the detection of c-crack, critical bearing balls notches of a few hundred micrometers long, less than one micrometer wide and forming an arc. Results on nitride ceramic bearing balls are presented.

### **1. Introduction**

The inspection of spherical element is of major importance for application such as aeronautical bearing balls quality control. Those bearing balls were mainly made of steel, but are progressively replaced by ceramic (silicon nitride  $\text{Si}_2\text{N}_4$ ) which is lighter and offer a high resistance level. Due to this transition, former non-destructive inspection techniques based on eddy current no longer work and new approach must be evaluated to ensure no defects.

Researched abnormality in bearing balls are all located within the first millimetre under the ball surface, and can either be surface (open crack) or subsurface flaws. C-crack notches constitute the main researched kind. They are considered critical as their depth exceeds 50 $\mu\text{m}$  and are characterized by the length of the formed arc (from few hundred micrometer to millimeter).

Some approaches based on resonance spectroscopy were already studied (1,2,3,4), exploiting the acoustic spectrum variation induced by the presence of the flaws. Vibrational modes are excited thanks to a piezoelectric transducer or a laser and

detected by an interferometer. But due to the small amplitude of the variation compared to the variability of the measurement itself, the diagnosis remains difficult to establish.

Considering the size and location of the researched flaws, Rayleigh waves appear to be adapted for their detection. Lasers are an efficient mean to generate them, and do not require any coupling since the generation occurs directly into the medium. By using an interferometer for the detection part, the inspection setup become totally contactless, and the measurement is performed without disrupting the wave propagation.

Moreover, lasers enable to control the surface wave's directivity by shaping the generation spot to a line. Using this shaping, two Rayleigh waves are generated from either side of the line and propagate in opposite directions. This property is valid for plan surface generation, but can be transposed to spherical surface with additional parameters to consider.

D. Clorennec and D. Royer (5,6) studied the use of laser line source for Rayleigh wave's generation on a sphere, and established a relation giving the proper line source length in order to generate a collimated Rayleigh that propagates around the equator.

The present paper exposes a detection method that exploits this property to monitor the interaction of laser generated Rayleigh waves along their circumvolution around the equator of the sphere. Specific data processing is developed in order to extract flaw signature from the acquired signal, and are presented here. The method performances are evaluated for the detection of C-crack on 45mm diameter silicon nitride bearing balls.

## 2. Experimental setup

The experimental setup aims at generating collimated Rayleigh waves on the sphere, and monitoring their circumvolution around the equator using an interferometer. The setup is composed of:

- A generation laser Nd-Yag, 532nm, pulse duration of 7ns
- A detection laser Nd-Yag, 1064nm, coupled to a photorefractive crystal interferometer

Both generation and detection lasers are linked to the setup with optical fibers.

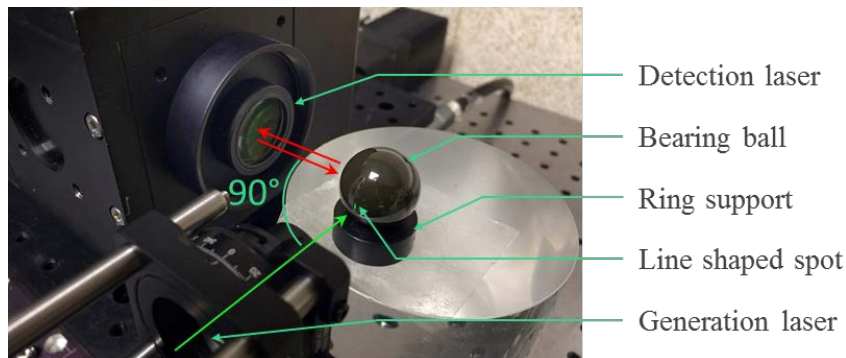


Figure 1. Experimental setup for the bearing ball inspection

The bearing ball is placed on a ring type support positioned so that the focal point of each laser is located on the sphere equator. Generation and detection laser are separated with an angle of  $90^\circ$ , which enables the best temporal separation of the two lateral Rayleigh wave-fronts.

The generation laser is shaped to a line source of  $200\mu\text{m}$  width, which length is adjustable thanks to a cylindrical lens. In order to generate collimated Rayleigh waves, the length is adjusted according to the relation  $L = \sqrt{2\pi a V_r \Delta}$  extracted from (5). The considered ceramic material displays a measured Rayleigh wave speed of  $V_r=5600\text{m/s}$ , the pulse duration of the generation laser is  $\Delta=7\text{ns}$  and the radius of the bearing ball is  $a=22.5\text{mm}$ , which gives a length of  $2.4\text{mm}$  for the line source.

The generation laser energy level is set in order to stay in the thermoelastic regime and avoid any damage on the surface. This was ensured by an optical control performed with a microscope on the region of impact.

Due to the lower sensitivity of a laser ultrasonic measurement compared to conventional piezoelectric transducer, the signal was averaged on 5000 laser shots. This significantly increases the signal to noise ratio, which is essential to be able to detect the signature induced by micrometric flaws.

An example of a recorded signal is presented on Figure 2. It displays the successive wave-fronts of the two Rayleigh waves circumvolving in opposite directions around the equator. This measurement reveals to be very reproducible in such manner that two distinct measurements on the same ball superimpose with less than 10% variation.

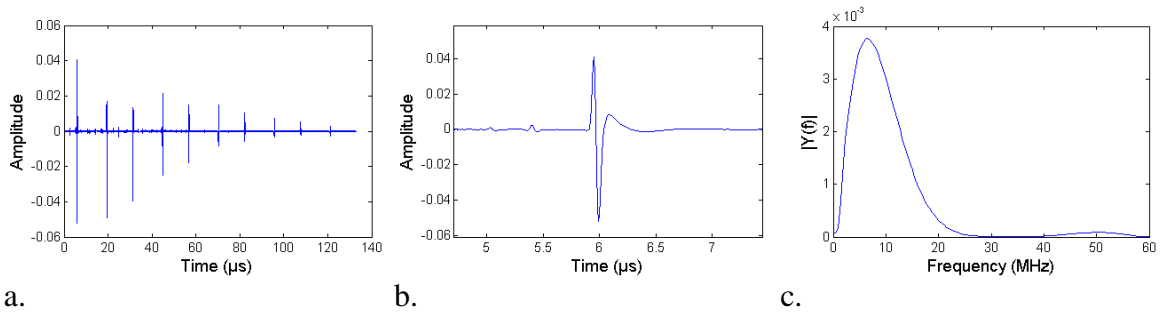


**Figure 2. Signal recorded on a 45mm diameter bearing ball. (a) Overall signal enlightening the two circumvolving Rayleigh waves. (b) Close-up on first Rayleigh wavefront. (c) Spectrum of first Rayleigh wavefront**

This observation leads to the following reasoning: if the bearing ball is flawless, then it can be considered as perfectly spherical and thus the previously recorded signal should not be dependent of the ball configuration on the support.

Conversely, if a flaw is present in the ball, the flaw signature will change for any different configuration of the ball and may be visible by comparison.

### 3. Developed approach for detection and experimental results

The previously exposed reasoning was evaluated on a bearing ball presenting a 550 $\mu$ m C-crack. The acoustical response of the bearing ball was measured for several positions of the C-crack on the equator, since the equator is the only insonified area.

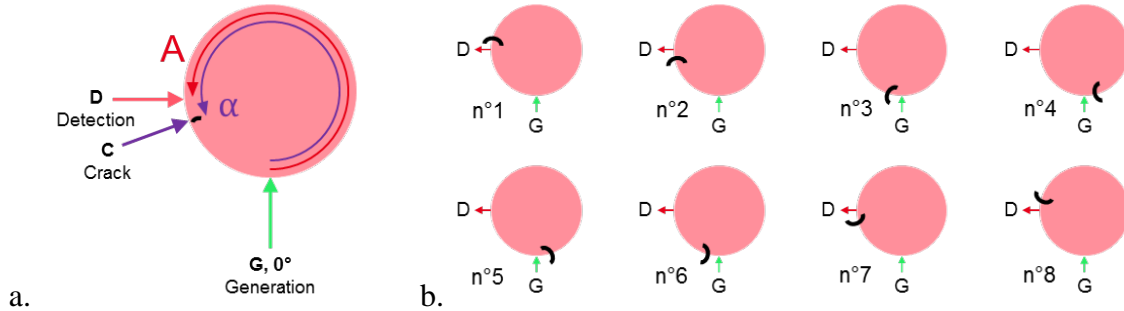


**Figure 3. (a) Defining generation, detection and crack positions on a polar coordinate system on the sphere equator. (b) Selected C-crack positioning on the sphere equator for the acquisition set**

A comparison of all obtained Ascan is presented Figure 4. The variation induced by the flaw signature is visible but its relative amplitude is 40 to 50dB below the amplitude of the Rayleigh wavefront. Thus, any attempt to isolate this signature by direct subtraction will not work despite the good measure reproducibility.

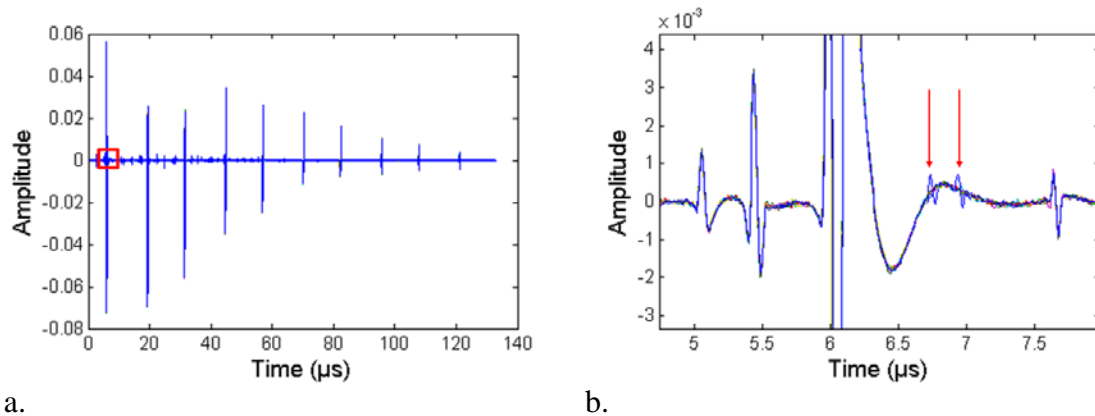


**Figure 4. (a) Superposition of all the 8 ascan corresponding to the 8 positions of the C-crack. (b) Close-up on the signal to enlighten flaw signature (red arrows) and its relative amplitude**

Likewise, a correlation computation will not be sufficiently sensitive to this small variation, even with a shifting window.

The developed approach relies on the study of the theoretical time of flight of the signature of a flaw located on the equator. If we consider a sectional view of the ball on the equator, we can define a polar coordinate system where the generation point, the detection point and the flaw will all be located on the circle of radius the radius of the ball (Figure 3.a).

If we now assume that the generation is at  $\theta=0^\circ$ , the position of the flaw is then defined by the angle  $2\pi\alpha$  and the detection by the angle  $2\pi A$ . Likewise, the time needed for a Rayleigh wave to perform a round trip around the equator is defined by:

$$T = \frac{2\pi a}{V_r}$$

Then, considering two Rayleigh wavefronts generated at  $t=0$ s on generation point and circumvolving in opposite direction around the equator, they may interact with the flaw resulting in a transmitted wave and a reflected wave. Those resulting waves may also interact with the flaw, and so on. The study of the expected time of flight at the detection point of these wavefronts enlightens periodic patterns which fall into four schemes:

$$\begin{cases} [A + k]T, & k \geq 1 \\ [A + 2(\alpha - A) + k]T, & k \geq 0 \\ [1 - A + k]T, & k \geq 1 \\ [1 - A - 2(\alpha - A) + k]T, & k \geq 0 \end{cases}$$

Among those time of flight patterns, only two depend on the flaw position  $\alpha$ . The two others correspond to the times of flight that would be encountered in the case of a flawless ball.

Every time of flight is periodical, of period T. Moreover, it can be noticed that they are symmetrical to T: a same flaw will contribute at times X and T-X, also with a period T. This means a constructive summation of the flaw signature can be performed on the original signal to enhance the relative amplitude of the flaw signature. A new representation of the original signal is thus defined as following:

$$\forall t \in [0 - T[: \quad C(t) = \sum_{k=0}^{\infty} Ascan(t + kT)$$

The interval  $[0-T[$  can also be converted to an angular position thanks to the relation:

$$\alpha = 2\pi \frac{t}{T}$$

On this representation, the flaw signatures are more likely to add constructively whereas other signal will add destructively. The relative amplitude of the flaw signature will then increase.

This reasoning is only valid if the dispersion can be neglected, otherwise the wavefront will spread over time and it would not be possible to define a period T for the summation to be constructive. The frequency spectrum of the first Rayleigh wavefront (Figure 2) enlightens a central frequency of 6.5MHz with 150% Bandwidth. The corresponding  $ka$ , with  $a$  the radius of the sphere, is higher than 80, which is sufficient to neglect the effect of dispersion over the considered acquisition time (5).

The flaw signature may not be directly visible on the resulting  $C(t)$ , but is more likely to be identified by direct comparison with other  $C(t)$  acquired on the same ball. Considering a set of acquisition (as in Figure 3), a new representation is defined as follow:

$$S_i(t) = \sum_{j \neq i} C_i(t) - C_j(t)$$

These  $S_i(t)$  are plotted for the analysis. The results for the set of Figure 3.b are presented on Figure 5.a. As a comparison, the same set of acquisition was performed on a flawless ball and result data processing is presented on Figure 5.b.

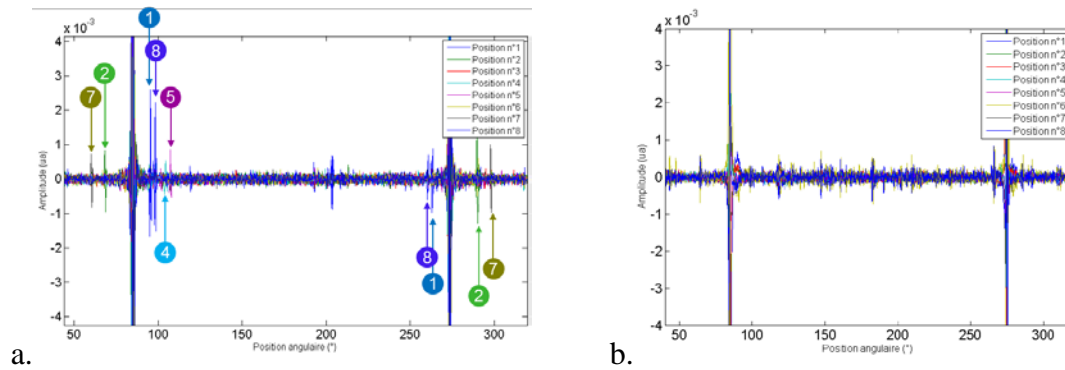


**Figure 5. (a) Signal processing result on the acquisition set with the 550µm C-crack bearing ball, the C-crack signature is enlightened for several flaw positioning. (b) Signal processing result on the reference bearing ball, with no C-crack**

On both Figure 5.a and Figure 5.b, two main peaks can be noticed at  $\theta=90^\circ$  and  $\theta=270^\circ$ . They correspond to the two Rayleigh wavefronts that circumscribe in opposite direction around the equator, with no interaction with flaw. Their positions reflect the fact that generation and detection are separated by an angle of  $90^\circ$ . It also illustrates the symmetry property introduced before, as  $270 = 360 - 90$ .

On Figure 5.a, additional peaks can be noticed and are associated to the C-crack signature for position 1, 2, 4, 5, 7, 8. This is confirmed by the fact that the symmetrical signature is also observed for positions 1, 2, 7, 8, as expected in previous reasoning.

C-crack position 3 and 6 do not produce any visible signature. Those flaw positions correspond to configuration where the flaw is too far away from detection and cause scattering of the interaction signature before it can be detected. It is also true for positions 4 and 5 for which a signature is visible, but not the symmetrical.

Considering the flawless ball, it cannot be noticed any peak with significant amplitude that also have a symmetrical, confirming the fact that the data process can discriminate healthy ball from faulty one. Nevertheless, the signal to noise ratio remains low and might be subject to bad interpretation.

In order to improve the signal to noise ratio of flaw signature, and reduce the amplitude of artefact, an additional signal processing was developed. It is based on the properties of the chosen representation  $S_i(t)$ :

$$\forall t \sum_i S_i(t) = 0$$

And on the fact that if a flaw exists, it induces an increase of the standard deviation at a given time  $t$ . The mathematical development will not be described here, but the application of this new processing is presented on Figure 6.

Figure 6 shows a significant reduction of the noise level as well as an increase of flaw signature amplitude. Considering the flawless ball, the new data processing also significantly decreases the noise level and confirms the fact that no flaw signature is visible.

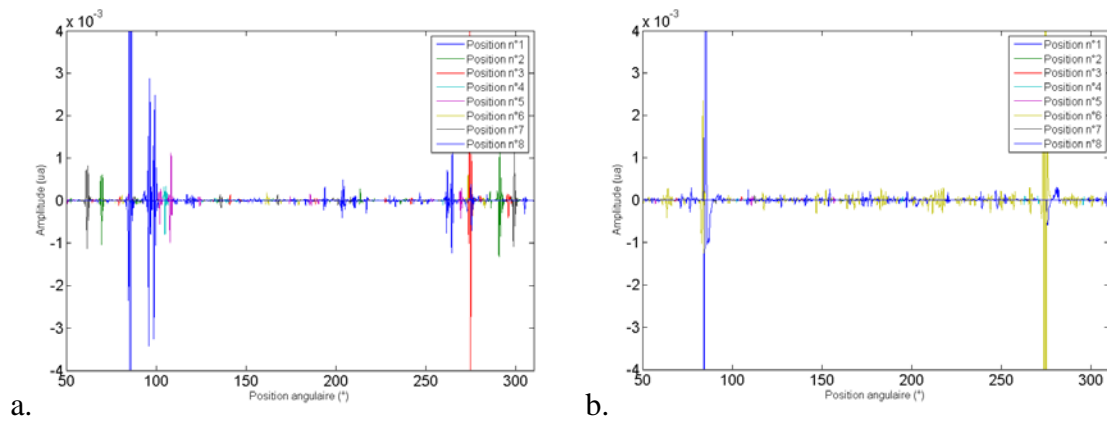


**Figure 6. (a) Enhanced signal processing result on the acquisition set with the 550µm C-crack bearing ball. (b) Enhanced signal processing result on the reference bearing ball, with no C-crack**

## 4. Conclusions

Based on the monitoring of collimated circumvolving Rayleigh waves generated and detected by laser, the present study proposes a methodology to identify very small surface or subsurface flaw on a sphere.

The methodology is based on the periodicity of the expected time of flight of a flaw signature when it is located on the equator. This property led to a new representation of the temporal signal which induces a constructive summation of the flaw signature, whereas others components tend to add destructively.

On the basis of this representation, a comparative methodology of signal acquired on the same ball was proposed. This method enabled the detection of a 500µm C-crack, despite a noise level that could interfere with proper diagnosis. However, the symmetry property of a flaw signature can be used to discard most of the artefacts. Nevertheless,

some flaw signatures remain low compared to the noise level and may be interpreted as artefact as well.

An enhancement of the data processing algorithm was introduced, though not described here, and led to significant reduction of the noise level, as well as an increase of flaw signature amplitude. This additional processing increases the confidence in establishing a diagnosis.

Although not presented here also, the method was tested on other bearing balls presenting C-crack. The signal processing has successfully detected the signature of a 750 $\mu$ m C-crack as well as a 350 $\mu$ m C-crack.

Nevertheless, the methodology has requirements in order to properly work. First, the ball radius and the generated frequencies must be high enough for the dispersion to be neglected. Second, the initial signal must present very high signal to noise ratio and be reproducible. It implies for the ball to be perfectly spherical and homogeneous, and also to average data on a high number of acquisitions.

This last aspect can lead to considerable acquisition time since laser ultrasonic system does not generally exceed 100Hz. A single set of 8 Ascan cover only a small fraction of the ball surface and an overall scanning of the ball would require several thousand of them. This causes the acquisition time to be counted in hours, which is not practically acceptable for an in-line monitoring.

## References and footnotes

1. High frequency ultrasonic detection of C-crack defects in silicon nitride bearing balls, F. Deneuille, M. Duquennoy, Ouaftouh, M. Ourak, F. Jenot, S. Desvaux, *Ultrasonics* 49 (2009) 89–93.
2. Non-destructive testing of ceramic balls using high frequency ultrasonic resonance spectroscopy, S. Petit, M. Duquennoy, M. Ouaftouh, F. Deneuille, M. Ourak, S. Desvaux, *Ultrasonics* 43 (2005) 802–810.
3. Laser ultrasonics detection of an embedded crack in a composite spherical particle, Ahmed Amziane, Mohamed Amari, Denis Mounier, Jean-Marc Breteau, Nicolas Joly, Julien Banchet, David Tisseur, Vitalyi Gusev, *Ultrasonics* 52 (2012) 39–46.
4. Evaluation on Micro Cracks in Ceramic Bearing Balls by Using the Floating Resonance of Surface Acoustic Waves, Hideo Cho, Kouichi Komatsu, Satoru Ishikawa, Kiyoshi Tanimoto, Hirokazu Takii and Kazushi Yamanaka, *Jpn. J. Appl. Phys.* Vol. 42 (2003) pp. 3176–3179.
5. Investigation of surface acoustic wave propagation on a sphere using laser ultrasonics, D. Clorennec and D. Royer, *Applied Physics Letters* Volume 85, Number 12, 2014.
6. Observation of diffraction-free propagation of surface acoustic waves around a homogeneous isotropic solid sphere, Yusuke Tsukahara, Noritaka Nakaso, Hideo Cho, and Kazushi Yamanaka, *Applied Physics Letters* 77, 2926 (2000).